Neurotherapeutics (2021) 18:889–904
https://doi.org/10.1007/s13311-020-00998-0

ORIGINAL ARTICLE

Selective Immunomodulatory and Neuroprotective Effects of a NOD2 Receptor Agonist on Mouse Models of Multiple Sclerosis

Adham Fani Maleki[1] · Giulia Cisbani[1] · Nataly Laflamme[1] · Paul Prefontaine[1] · Marie-Michele Plante[1] · Joanie Baillargeon[1] · Manu Rangachari[1] · Jean Gosselin[2] · Serge Rivest[1]

Accepted: 18 December 2020 / Published online: 21 January 2021

Abstract

The significance of monocytes has been demonstrated in multiple sclerosis (MS). One of the therapeutic challenges is developing medications that induce mild immunomodulation that is solely targeting specific monocyte subsets without affecting microglia. Muramyl dipeptide (MDP) activates the NOD2 receptor, and systemic MDP administrations convert Ly6C^{high} into Ly6C^{low} monocytes. Here, we report selective immunomodulatory and therapeutic effects of MDP on cuprizone and experimental autoimmune encephalomyelitis (EAE) mouse models of MS. MDP treatment exerted various therapeutic effects in EAE, including delaying EAE onset and reducing infiltration of leukocytes into the CNS before EAE onset. Of great interest is the robust beneficial effect of the MDP treatment in mice already developing the disease several days after EAE onset. Finally, we found that the NOD2 receptor plays a critical role in MDP-mediated EAE resistance. Our results demonstrate that MDP is beneficial in both early and progressive phases of EAE. Based on these results, and upon comprehensive basic and clinical research, we anticipate developing NOD2 agonist–based medications for MS in the future.

Key Words Monocytes · Microglia · Multiple sclerosis · EAE · NOD2 receptor · Cuprizone

Introduction

MDP is a bioactive fragment containing minimal peptidoglycan motif from most gram-negative and gram-positive bacteria [1] and is used as an adjuvant in different vaccine formulations [2]. MDP activates the NOD2 pattern recognition receptor, which is the essential receptor for the innate immune response to MDP [1, 3].

NOD2 receptor is a cytosolic protein and member of the NOD-like receptor family involved in the control of innate immune functions, especially the pattern recognition receptors (PRRs). [1]. Studies have reported different and contradictory roles of NOD2 in either promoting or inhibiting inflammation [4, 5], and also participating in the modulation of T-cell functions [6]. Strong expression of NOD2 receptor has been demonstrated in cells of myeloid origin, such as monocytes and macrophages [7].

In humans, three monocyte subsets are characterized based on CD14 and CD16 expression levels. Classical ($CD14^{++}CD16^{-}$), intermediate ($CD14^{++}CD16^{+}$) and nonclassical ($CD14^{+}$ $CD16^{++}$) subsets [8]. In mice, using a combination of cell surface markers, proinflammatory monocytes are characterized as ($CX3CR1^{low}CCR2^{+}Ly6C^{high}$), whereas patrolling monocytes are defined as $CX3CR1^{high}CCR2^{-}Ly6C^{low}$ cells [9, 10]. In pathological situations, monocytes gain a nonredundant function, such as pro- and anti-inflammatory activities and tissue repair, to name a few, that cannot be replaced by macrophages and conventional dendritic cells [9]. Proinflammatory monocytes (also referred to as inflammatory monocytes; Ly6C^{hi} monocytes) extravasate in inflamed tissues and contribute to local inflammation. On the contrary, anti-inflammatory monocytes (also referred to as patrolling monocytes; Ly6C^{low} monocytes) establish the resident regulatory patrolling monocyte population [9, 11]. Ly6C^{low} monocytes mediate anti-inflammatory responses, as the population of resident phagocytes, they have been shown to remove cellular debris and enhance tissue repair [11].

✉ Serge Rivest
serge.rivest@crchudequebec.ulaval.ca

[1] Neuroscience Laboratory, CHU of Quebec Research Center and Department of Molecular Medicine, Faculty of Medicine, Laval University, 2705 Laurier Boul., Quebec City, QC G1V 4G2, Canada

[2] Laboratory of Innate Immunity, CHU of Quebec Research Center and Department of Molecular Medicine, Faculty of Medicine, Laval University, 2705 Laurier Boul., Quebec City, QC G1V 4G2, Canada

MS is a demyelinating inflammatory disease characterized by T cell–driven autoimmune attack against CNS-derived antigens such as myelin [12]. However, mononuclear phagocytes are the dominant cell type that is abundantly found in active and chronic MS and EAE lesions [13], and accumulating evidence underlines a crucial role of monocytes in MS progression [14, 15]. In particular, recent studies reported that Ly6C^{high} monocytes are the most important cell type in EAE CNS lesions [16, 17]. The severity of EAE depends on Ly6C^{high} monocytes as they expand exponentially before EAE onset and play crucial roles in the effector phase [18]. In contrast, a recent study demonstrated that nonclassical CD14^{+} CD16^{++} monocytes (counterpart to murine patrolling monocytes) are depleted in the circulation of patients with MS. Indeed, the ratio of nonclassical CD14^{+} CD16^{++} monocytes to classical CD14^{++} CD16^{-} monocytes was lower in cerebrospinal fluid of patients with MS compared to the control group [19]. In parallel, the crucial role of monocyte-derived macrophages in the regulation of neuroinflammation in MS and EAE has also been demonstrated [20].

Recently, we have reported therapeutic effects of MDP-mediated immune modulation on monocyte subsets in a mouse model of Alzheimer's disease [21]. In the current study, we investigated whether MDP could influence neuropathology of mouse models of MS by regulating monocyte cell subsets. We performed *in vivo* studies of immunomodulatory effects of MDP in two mouse models of MS (cuprizone and EAE). We found that MDP administrations in both MS models convert Ly6C^{high} into Ly6C^{low} monocytes, but there were no significant changes in demyelination levels in the cuprizone model. On the other hand, peripheral MDP administrations in EAE delayed the onset of disease, improved clinical scores, and reduced leukocyte infiltration into the CNS before the onset of the disease. Of great interest is the strong beneficial effect of the MDP treatment in mice already developing the disease several days after the EAE onset. Using NOD2$^{-/-}$ mice, we found NOD2 receptor plays a critical role in MDP-dependent immune modulation and EAE resistance.

Material and Methods

Animal Care

All protocols were performed according to the Canadian Council on Animal Care guidelines, as administered by the Laval University Animal Welfare Committee. All experiments were approved by the local committee. All efforts were made to avoid their suffering. All mice were maintained in a pure C57BL/6J background, bred in house, and newborn pups were genotyped with PCR as advised by Jackson Laboratory protocols. All animals were housed up to four per cage in a temperature- and light-controlled room (12-h light cycles from 7 am to 7 pm) and were fed (mouse chow) and allowed to drink water ad libitum. All mice were monitored for health status, including weight loss throughout all experimental protocols.

Cuprizone Diet and MDP Treatment

Thirty 6- to 8-week-old C57BL/6J male mice were fed with either normal chow ($n = 10$) or the cuprizone-supplemented chow ($n = 20$). 0.2% wt/wt the cuprizone (bis-cyclohexylidene hydrazide; Sigma–Aldrich) was mixed with regular ground chow and fed to experimental animals for 5 weeks. The food was changed every 2 days, and food intake was monitored throughout the protocols. Control animals were fed with regular ground chow and manipulated as often as cuprizone-fed mice. During the 5 weeks of the diet, mice were injected three times per week with either MDP (Cat# tlrl-mdp, InvivoGen) diluted in saline (10 mg/kg), or vehicle (saline 0.9%), intraperitoneal (i.p.) injection (Fig. 1a).

Behavioral Analysis of Cuprizone Mice

Nesting behavior test in the groups of cuprizone and normal food mice was performed based on sore of 1–5 as described by [22]. ANY-mase system was used to perform an open field test in order to record and analyze each mouse individually in all experimental groups as described by [23].

EAE Induction and MDP Treatment

One hundred twenty-one 10-week-old male C57BL/6J mice, as well as twelve 10-week-old male NOD2$^{-/-}$ mice, were used to study the impact of MDP treatment in the EAE model. EAE was induced by subcutaneous injection of mice with 2 × 100 μl of an emulsion containing CFA (complete Freud adjuvant), 1 mg *Mycobacterium tuberculosis* extract H37-Ra (Difco), and 100 μg MOG35–55 (MEVGWYRSPFSRVVHLYRNGK) along with an i.p. injection of 200 ng pertussis toxin (PTX) (Sigma–Aldrich) on day 0 (immunization phase). On day2, mice received a second i.p. injection of PTX, followed 24 h later (or after the disease onset, depends on the protocols) by the first injection of MDP or NG–MDP (Cat# tlrl-gmdp, InvioGen) diluted in saline (10 mg/kg) or vehicle (saline 0.9%). MDP or vehicle was administered every 2 days. Animals were monitored daily for development of EAE according to the following criteria: 0, no disease; 1, decreased tail tone; 2, hind limb weakness or partial paralysis; 3, complete hind limb paralysis; 4, front and hind limb paralysis; 5, moribund state. To evaluate circulating immune cell subsets, blood samples were collected from the submandibular vein and kept in ethylenediaminetetraacetic acid (EDTA) coated vials (Microvette® K3E, Sarstedt, Montreal, QC, Canada) 9 and 21 days after immunization. Mice were then sacrificed at 21 days

after immunization. To study the cerebral subsets of immune cells, mice were sacrificed 12 days after immunization.

Flow Cytometry

Blood samples were collected from the submandibular vein and kept in EDTA coated vials on a rotator for < 1 h. Flow cytometry analysis was performed as described previously for extracellular [24, 25], and for intracellular staining [26]. FACS and data acquisition were performed using SORP LSR II and FACSDiva software (both from BD). Results were analyzed with the FlowJo software (v10.5.3). For details on flow cytometry experiments, see Electronic Supplementary Material (Supplementary Experimental Procedures section). Gating strategy for leukocyte quantification in blood and the CNS are presented in Electronic Supplementary Material (Fig. S6 and S7).

CNS Flow Cytometry

EAE mice were deeply anesthetized via an i.p. injection of a mixture of ketamine hydrochloride and xylazine and then perfused intracardially with ice-cold DPBS. CNS were extracted and immediately homogenized for cell isolation. The same blood sample panels were used for extracellular and intracellular staining. FACS and data acquisition were performed using SORP LSR II and FACSDiva software (both from BD). Results were analyzed with the FlowJo software (v10.5.3). For details on flow cytometry experiments, see Electronic Supplementary Material (Supplementary Experimental Procedures section).

Postmortem Analysis

Histochemical Immunostaining

Brain sections were washed four times for 5 min in KPBS and then blocked in KPBS containing 1% BSA, 4% NGS, and 0.4% Triton X-100. The slices were then incubated overnight at 4 °C with the primary antibody anti-Olig2 (rabbit, 1:1000; Millipore) and anti-Iba-1 (rabbit, 1:1000; DAKO). After washing the sections four times for 5 min in KPBS, tissues were incubated in the appropriate secondary antibody (biotinylated goat anti-rabbit IgG; 1:1500, Vector Laboratories) 2 h at room temperature. Following further washes in KPBS and 1-h-long incubation in the avidin–biotin–peroxidase complex (ABC; Vector Laboratories) to reveal the staining, the sections were then incubated in 3,30-diaminobenzidine tetrahydrochloride (DAB; Sigma). The sections were mounted onto Micro Slides Superfrost plus glass slides, dehydrated, and then coverslipped with DPX mounting media.

Black Gold Staining

Brain sections were washed three times for 10 min in cold KPBS and mounted onto Superfrost slides glass slides. The slides were prewarmed 30 min at 65 °C on a slide warmer, washed once with warm KPBS, followed by incubation in 0.3% Black Gold (Sigma–Aldrich) diluted into 0.9% NaCl for 30 min. After this time, slides were washed in warm KPBS and then in warm sodium thiosulfate for 3 min and then transferred into KPBS. All the steps were performed at 65 °C. Finally, the slides were dehydrated in alcohol, cleared in xylene, and coverslipped with DPX. Using a Qimaging camera, 8-bit grayscale TIFF images of the regions of interest were taken in a single sitting for the cuprizone model, with the same gain/exposure settings for every image. To quantify the demyelination/myelination level, these images were imported into ImageJ, and myelination of a given area was measured as the surface proportion of staining intensity above a determined threshold.

In Situ Hybridization

In situ hybridization was performed as described previously [27] on all brain sections, starting from the end of the olfactory bulb to the end of the cortex. ^{35}S-labeled complementary RNA probes for TREM2, TLR2, and PDGFRα were used for *in situ* hybridization. Films were then scanned using an Epson Perfection v850 Pro scanner supported by the SilverFast software (version 8.8.Or6). The area and intensity of positive hybridization signals were densitometrically measured on all brain sections using ImageJ software (Version 2.0.0-rc-43/1.51n). Each value was corrected for background signal by subtracting the OD value measured at a brain area devoid of positive signal (For a detailed protocol, see the reference [28].

Statistical Analysis

Data are expressed as the mean ± SEM. Comparison between two groups was conducted using post hoc unpaired *t* tests. Comparisons between more than two treatment groups were conducted using either one-way analysis of variance (ANOVA) or two-way repeated-measures ANOVA, followed by appropriate multiple comparison tests. Disease incidence was analyzed by log–rank (Mantel–Cox) test. Values were statistically significant if $p < 0.05$. All analyses were performed using GraphPad Prism Version 7 for Windows (GraphPad Software, San Diego, CA, USA). All panels were assembled using Adobe Photoshop CS5 (version 12.0.4) and Adobe Illustrator CS5 (version 15.0.2).

Results

MDP Administration in Cuprizone-Induced Demyelinating Mouse Model of MS

Systemic MDP Administrations Modulate Circulating Monocyte Subsets in Mice Fed with the Cuprizone-Supplemented Diet

Microglia and monocyte-derived macrophages coordinate the remyelination process via phagocytosis and inflammatory responses [24, 29]. In this regard, a previous study from our group showed the phagocytic feature of Ly6C^{low} monocytes in the CNS [30]. In parallel, Lessard and colleagues recently reported that peripheral MDP administrations convert inflammatory Ly6C^{high} monocytes into Ly6C^{low} patrolling monocytes [25]. Therefore, we first examined immunomodulatory effects of MDP in the cuprizone model. Wild type mice were fed with normal chow or cuprizone-supplemented chow for 5 weeks, and the pick of demyelination is observed between 4 and 5 weeks of the diet. During the 5 weeks of cuprizone intoxication, mice received MDP (10 mg/kg/i.p.) or saline injections twice a week (Fig. 1a). Mice were followed-up throughout the experimental course to evaluate food intake as well as body weight. Similar to our recent publication [31], we did not observe differences in food intake in any group; however, both groups fed with cuprizone-supplemented chow exhibited weight loss (Fig. 1b). At the end of the cuprizone intoxication, blood was collected, and monocyte populations were examined (Fig. 1c and d). Compared to the control groups, MDP treatments showed a significant increase in the percentage of Ly6C^{low} monocytes and significantly decreased in the percentage of Ly6C^{high} monocytes in both groups of mice

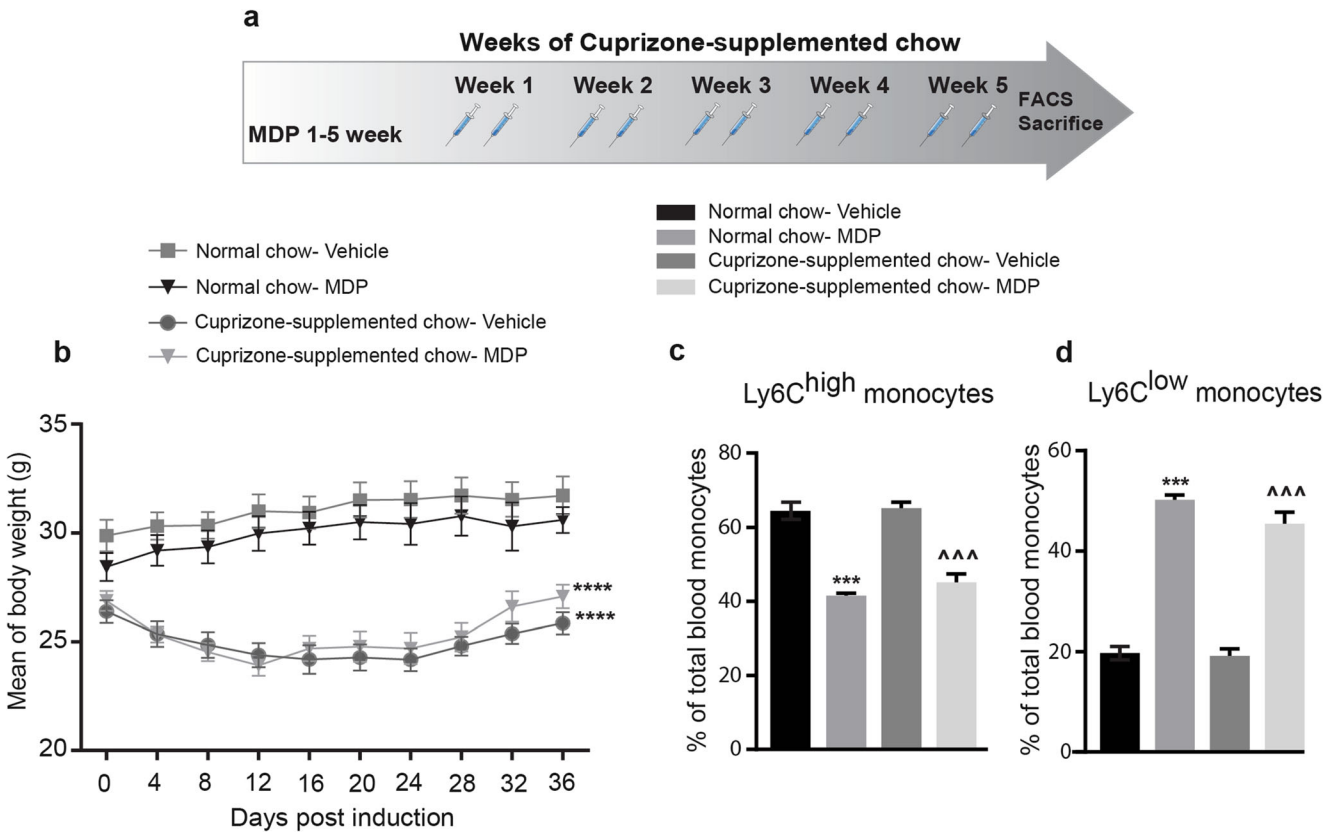

Fig. 1 Systemic MDP administrations shift monocyte subsets towards Ly6C^{low} monocytes in the cuprizone model. (a) Representative of the timeline of weeks of cuprizone-supplemented chow and MDP administration. $n = 5$ mice/group used in treatment and control groups in normal food, and $n = 10$ mice/group used in treatment and control groups in cuprizone-supplemented diet. (b) Mean of body weight changes following treatment with vehicle or MDP in normal food and cuprizone-supplemented diet groups. Data are expressed as the means ± SEM; ****$P < 0.0001$, two-way ANOVA followed by Dunnett's multiple comparisons test. (c) Percentage of blood inflammatory Ly6C^{hi} monocytes following treatment in normal food and cuprizone-supplemented diet groups as measured by FACS. Data are expressed as the means ± SEM; ***$P <$ or = 0.0001 *versus* normal chow–vehicle, ^^^$P <$ or = 0.0001 *versus* cuprizone-supplemented chow–vehicle, one-way ANOVA with Tukey's multiple comparisons test. (d) Percentage of blood Ly6C^{low} patrolling monocytes following treatment in the experimental groups. Data are expressed as the means ± SEM; ***$P <$ or = 0.0001 *versus* normal chow–vehicle, ^^^$P <$ or = 0.0001 *versus* cuprizone-supplemented chow–vehicle, one-way ANOVA with Tukey's multiple comparisons test

fed with cuprizone-supplemented chow or normal chow. In particular, following MDP administrations, the initial percentage of Ly6C^{high} monocytes which was about 60% in both normal food and cuprizone groups decreased to 40%. In parallel, the percentage of Ly6C^{low} monocytes (20%) increased and reached approximately 50% in both groups (Fig. 1c and d).

Before ending the protocol, behavioral tests were performed to explore if the demyelination level induced by cuprizone intoxication was associated with neurological alterations. We observed that the demyelination level was not reflected in behavioral tests, including nesting behavior, and open field tests, in the experimental groups (Fig. S1A, S1B, and S1C).

Five Weeks of Systemic MDP Administration Does Not Affect the Remyelination and Brain Inflammation in the Cuprizone Model

Next, we investigated if the MDP-mediated immune regulation could affect the demyelination at the histological level. Cuprizone intoxication leads to myelin loss in brain white matter. The corpus callosum, being the largest white matter region of the brain, is particularly susceptible to cuprizone. We performed a Black Gold II staining in the brain tissue from mice that were fed with cuprizone-supplemented chow and were treated with MDP or saline as well as corresponding normal chow groups (Fig. 2a). Because more severe myelin

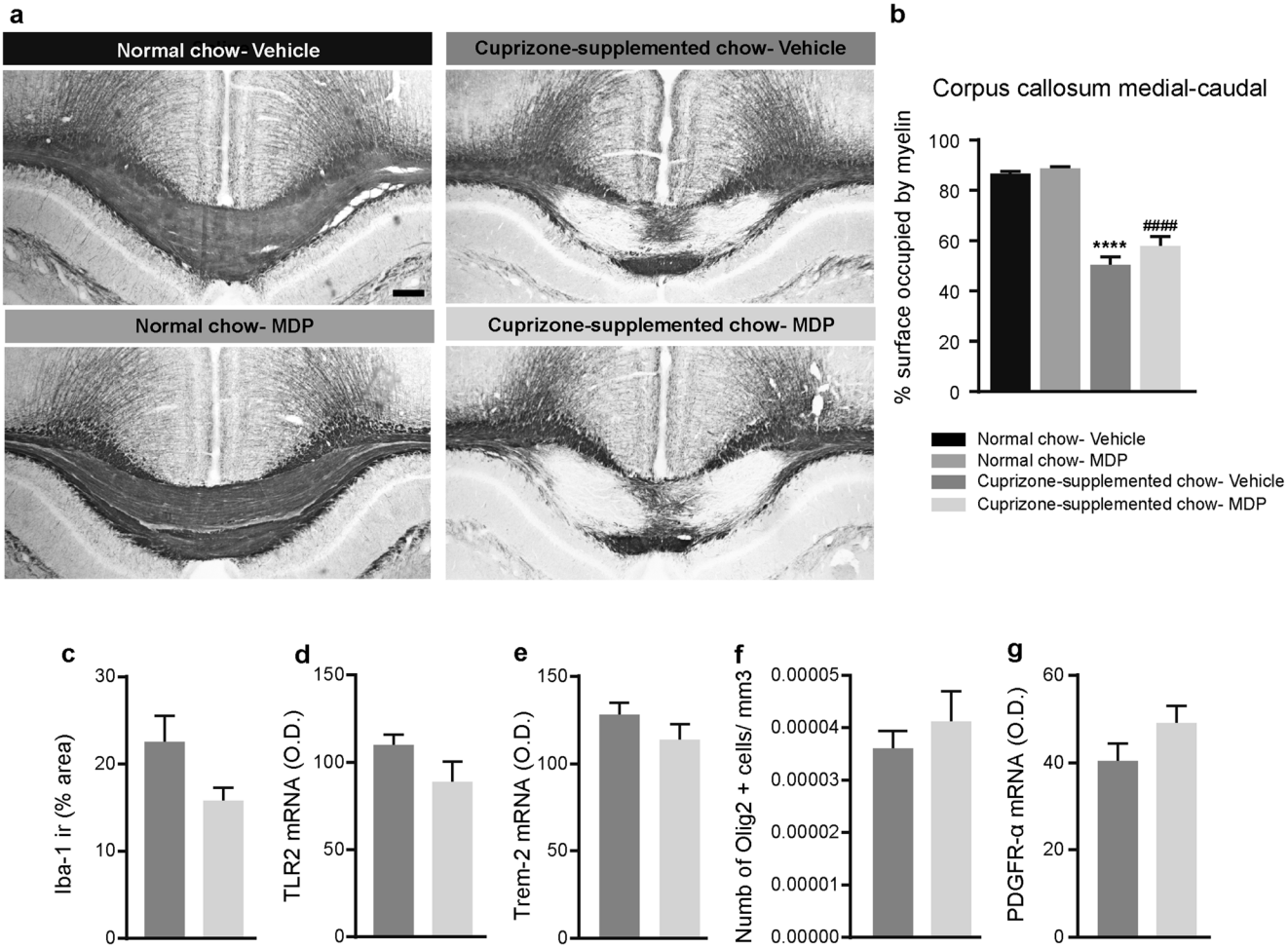

Fig. 2 MDP treatment did not significantly modulate remyelination levels, microglia activation, and inflammation in the CNS of cuprizone-fed mice. (a) Representative of Black Gold II staining of the medial-caudal area of the corpus callosum in normal food and cuprizone-supplemented diet. $n = 5$ mice/group in treatment and control groups in normal food, and $n = 10$ mice/group in treatment and control groups in cuprizone-supplemented diet. (b) Representative measuring of the medial-caudal area of the corpus callosum occupied by myelin in normal chow (vehicle and MDP) and cuprizone-supplemented chow (vehicle and MDP) groups. Data are expressed as the means ± SEM; $^{****}P < 0.0001$ *versus* normal chow–vehicle, $^{\#\#\#\#}P < 0.0001$ *versus* normal chow-MDP, one-way ANOVA with Tukey's multiple comparisons test. (c) Iba1 was immunostained on the medial-caudal area of the corpus callosum from cuprizone–vehicle and cuprizone–MDP mice. The area covered by Iba1^{+} staining was measured using a stereological procedure. (d) and (e) *In situ* hybridization signal of TLR2 and TREM2 mRNA in the medial-caudal area of the corpus callosum from cuprizone–vehicle and cuprizone–MDP mice. (f) Representative number of Olig2-immunoreactive staining (olig2^{+} cell/μm^{3}) in medial–caudal area of the corpus callosum from cuprizone–vehicle and cuprizone–MDP mice. (g) PDGFRα mRNA hybridization signal in the medial-caudal area of the corpus callosum of cuprizone–vehicle and cuprizone–MDP mice

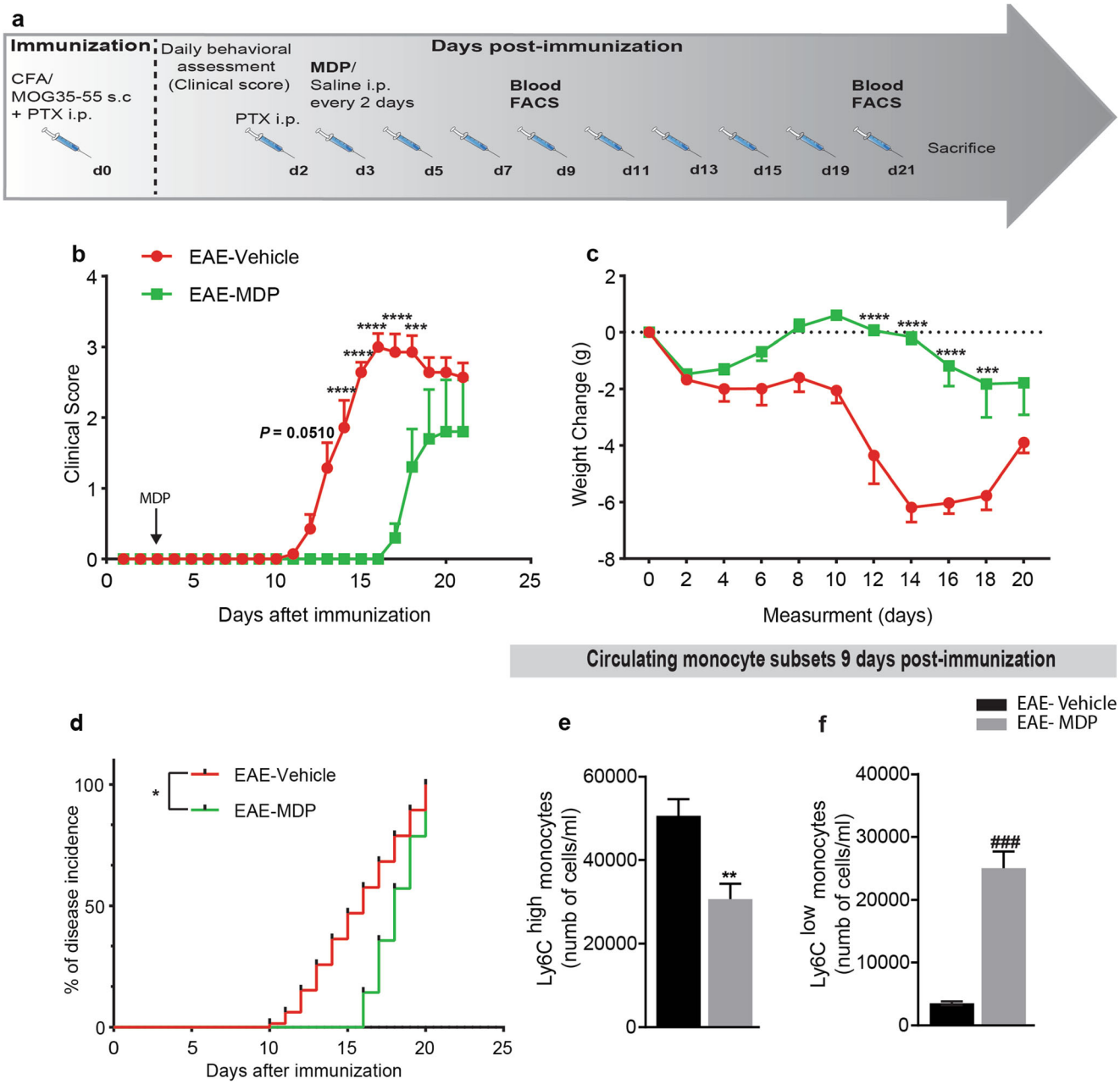

Fig. 3 Mice were highly resistant to EAE onset via shifting monocyte subsets towards Ly6C^{low} monocytes in response to the MDP treatment. (a) Representative timeline of the entire protocol, including EAE inducing, MDP administrations, and FACS analysis in mice treated with vehicle ($n = 7$) or MDP ($n = 7$). (b) Clinical scores of mice treated with vehicle or MDP were determined daily after immunization. Data are expressed as the means ± SEM; $^{****}P < 0.0001$, $^{***}P = 0.0008$, two-way ANOVA followed by Tukey's multiple comparisons test. (c) The variation of body weight has been expressed compared to the day of EAE induction (day 0) as mean ± SEM; $^{****}P < 0.0001$, $^{***}P = 0.0001$, two-way ANOVA followed by Tukey's multiple comparisons test. (d) Percentage of disease incidence in mice treated with vehicle or MDP. Data are expressed as the means ± SEM; $^{*}P = 0.02$, log–rank (Mantel–Cox) test. (e) and (f) Absolute count of blood Ly6C^{hi} and Ly6C^{low} monocytes respectively following treatment with vehicle or MDP in EAE mice as measured by flow cytometry 1 week after MDP injections (9 days after immunization). Data are expressed as the means ± SEM; $^{**}P < 0.05$ *versus* EAE–vehicle, $^{###}P < 0.0001$ *versus* EAE–vehicle, Student's *t* test

depletion is expected in the medial–caudal area of the corpus callosum [31], we analyzed this region by measuring the area occupied by myelin. We did not observe any differences in the myelin levels following MDP treatments (Fig. 2b). Concomitantly to the myelin loss, a robust microglial response is observed in the corpus callosum of mice that were intoxicated with cuprizone [31]. Following the observation of a shift in monocyte subsets in the

Table 1 EAE progression in WT mice treated with vehicle or MDP before EAE onset

Groups	Mean onset day	Mean score of maximal symptoms	Total days
EAE–vehicle	12.43 ± 0.36	3.0 ± 0.18	21
EAE–MDP	17.20 ± 0.20****	1.8 ± 0.73*	21

Representative of mean onset day and mean score of maximal symptoms, and total days for protocol in EAE–WT mice treated with saline or MDP. The treatments started before EAE onset. Data are presented as mean ± S.E.M. ****$P < 0.0001$, *$P = 0.04$, Student's t test

periphery, we sought to test whether MDP is capable of modulating microglial response. Following MDP treatment, mice that were exposed to cuprizone did not show any modulation of the microglial response (Fig. 2c), its activation measured by TLR2 expression (Fig. 2d) or its phagocytic activity measured by TREM2 levels (Fig. 2e). Finally, we evaluated whether MDP could affect the number of oligodendrocytes and oligodendrocyte progenitor cells, measured by the expression levels of Platelet-derived growth factor receptor α (PDGFRα). Similar to microglia results, we did not observe any difference between the groups treated with MDP or saline (Fig. 2f and g).

In summary, these results indicate that MDP administrations convert Ly6C^{high} to Ly6C^{low} monocytes in the cuprizone model. However, it does not impact either the brain myelination levels or the cerebral immune responses. These results suggest that MDP-mediated immune modulation on monocyte subsets in our experimental setup does not drive the remyelination process in mice exposed to cuprizone. Hence, we next investigated the MDP-dependent immunomodulation in the most commonly used animal model of MS in which systemic immune cells play a key role, the EAE model.

Systemic MDP Administration in EAE Mouse Model of MS

MDP Treatment Induces High Resistance to the Onset of EAE via Shifting Monocyte Subsets Towards Ly6C^{low} Monocytes

To address the potential therapeutic effect of MDP in the EAE model, we first assessed the EAE onset and severity in mice treated with MDP (EAE–MDP) or vehicle (EAE–vehicle). Mice were immunized by subcutaneous injection of a MOG peptide emulsified in complete Freund's adjuvant and accompanied by pertussis toxin (Fig. 3a). Animals were injected with MDP or saline 3 days after immunization. EAE–vehicle mice developed the disease as characterized by ascending paralysis [32]. Interestingly, EAE mice treated with MDP were protected from disease development as measured by clinical scores and weight change, demonstrating a delay on the day of onset (Fig. 3b and c). The disease incidence after EAE induction was significantly lower in EAE–MDP than EAE–vehicle (Fig. 3d). Additionally, we found a significant difference in mean onset days and mean maximum score in the treatment versus control groups (Table 1).

To explore the mechanisms underlying the protecting properties of MDP in the EAE model, blood leukocyte subpopulations were quantified before disease onset (1 week after MDP injections or 9 days after immunization) by flow cytometry (FACS) analysis. We observed that MDP administrations significantly increased Ly6C^{low} monocytes while decreasing Ly6C^{high} monocyte levels (Fig. 3e and f). Further analysis of FACS results obtained from the leukocyte populations showed a subtle tendency but not significant modulation of T-cell subsets (Fig. S2).

We next compared both groups of mice at 21 days after immunization when the EAE–vehicle group stabilized as demonstrated by clinical scores while the EAE–MDP group is in the acute phase. EAE mice that received MDP for 21 days exhibited a reduced number of Ly6C^{high} cells together with an increased number of Ly6C^{low} monocytes (Fig. S3). Altogether, these results suggest that MDP administrations after the onset of EAE keep shifting monocyte subsets towards Ly6C^{low} monocytes during the acute phase of EAE.

MDP Administrations Modulate Infiltration of Ly6C^{high}, Ly6C^{low} Monocytes, and Some Other Populations of Leukocytes into the CNS Before EAE Onset

We next determined whether the immunomodulatory effects of MDP on monocyte subsets, clinical scores, and the onset of EAE are correlated with the regulation of infiltrating cells into the CNS. Mice were immunized and injected with MDP every 2 days, as depicted by Fig. 4a. At 12 days after immunization, all EAE–vehicle mice had developed EAE, whereas the EAE–MDP group showed no clinical symptom (Fig. 4b–d and Table 2). At this time point, FACS analysis of the CNS confirmed the drastic reduction in the number of Ly6C^{high} together with the increase in Ly6C^{low} monocytes (Fig. 4e and f) as well as Ly6G^{+} cells (Fig. 4g).

Our results so far showed that MDP-mediated immune modulation on T-cell subsets in the periphery is not significant. Nevertheless, to determine whether these findings were also reflected in disease-specific T cells infiltrating into the CNS before the onset of EAE, we analyzed T-cell subsets. Infiltration of $CD3^+$, $CD4^+$, and

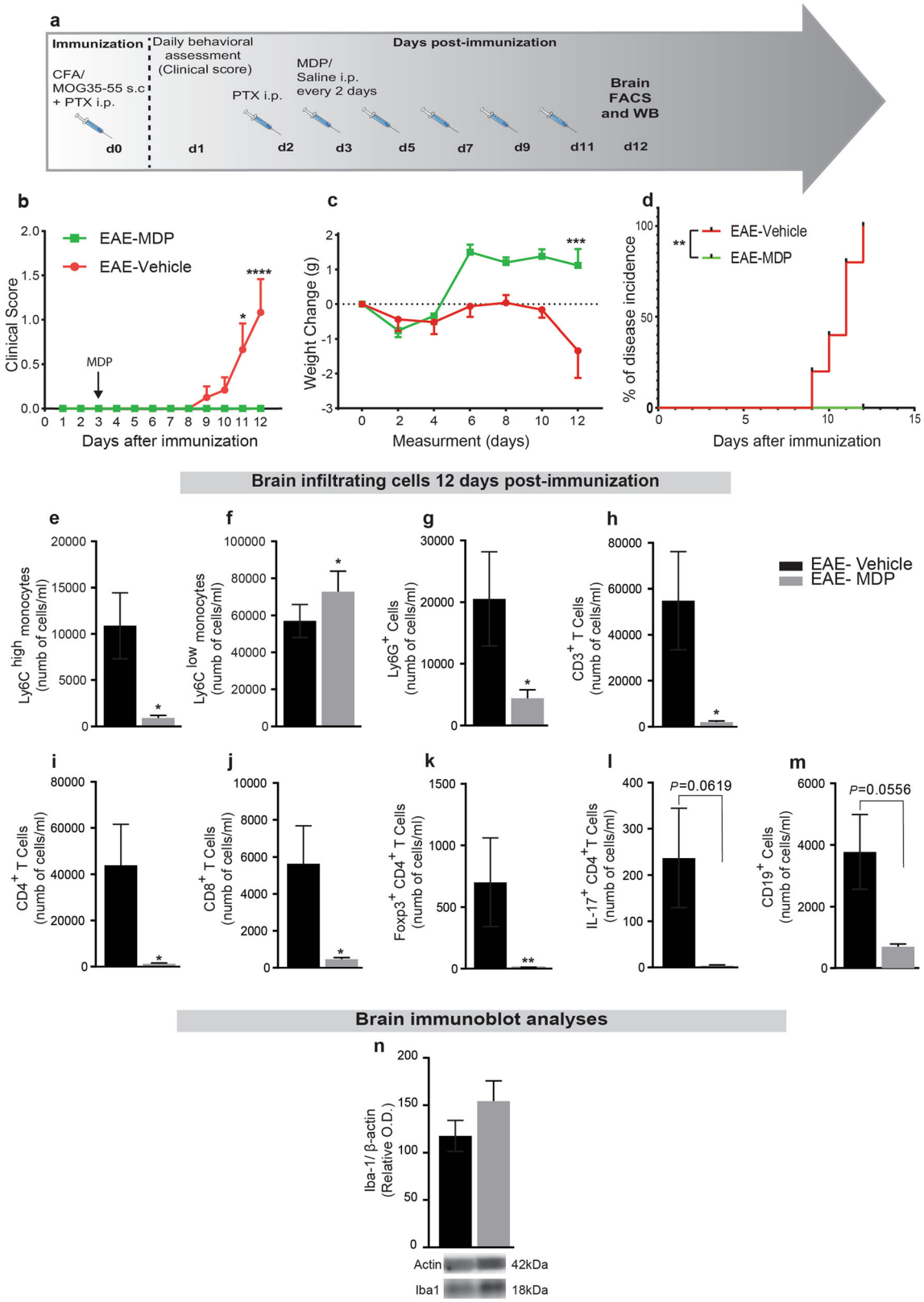

◀ **Fig. 4** MDP modulates monocyte subsets and infiltrating Ly6C^{hi}, Ly6C^{low} monocytes, T-cell subsets, Ly6G^{+} cells, and CD19^{+} cells in the CNS before the onset of EAE. (a) Representative timeline of the entire protocol, including inducing EAE, MDP administrations, and FACS analysis in WT mice treated with vehicle ($n = 10$) or MDP ($n = 9$). (b) Clinical scores of mice in the groups were determined daily after immunization. Data are expressed as the means ± SEM; $*P = 0.03$, $****P < 0.0001$, two-way ANOVA followed by Tukey's multiple comparisons test. (c) Body weight changes measured after immunization in the treatment and control groups. Data are expressed as the means ± SEM; $***P = 0.0001$, two-way ANOVA followed by Tukey's multiple comparisons test. (d) Percentage of disease incidence in mice treated with vehicle or MDP. Data are expressed as the means ± SEM; $**P = 0.002$, log–rank (Mantel–Cox) test. (e) and (f) Absolute count of CNS Ly6C^{hi} and Ly6C^{low} monocytes respectively following treatment with vehicle or MDP in EAE mice as measured by FACS 12 days after immunization. Data are expressed as the means ± SEM; $*P <$ or $= 0.02$, Student's t test. (g) Absolute count of CNS Ly6G^{+} cells following treatment in the experimental groups. Data are expressed as the means ± SEM; $*P <$ or $= 0.02$, Student's t test. (h)–(j) Absolute count of CNS CD3^{+}, CD4^{+}, and CD8^{+} T cells respectively following treatment in the experimental EAE groups measured by FACS. Data are expressed as the means ± SEM; $*P <$ or $= 0.04$, Student's t test. (k) and (l) Absolute count of CNS Foxp3^{+} CD4^{+}, and IL-17^{+} CD4^{+} T cells, respectively in the EAE mice measured by FACS 12 days after immunization. Data are expressed as the means ± SEM; $**P <$ or $= 0.007$, Student's t test. (m) Absolute count of CNS CD19^{+} cells following treatment with vehicle or MDP in EAE mice as measured by FACS 12 days after immunization. (n) Immunoblot analysis of Iba1 protein expression in the CNS showed no significant difference between groups

CD8^{+} T cells before the onset of EAE was significantly reduced in EAE–MDP compared to the EAE–vehicle group (Fig. 4h–j). At the same time point, the numbers of infiltrating Foxp3^{+} regulatory and IL-17^{+} CD4^{+} T cells into the CNS reduced in the MDP-treated group (Fig. 4k and l). In addition, CD19^{+} cells infiltrated into the CNS showed a strong tendency in the MDP-treated group compared to the control (Fig. 4m). Interestingly, IL-17^{+} CD8^{+} T cells were not detected at this time point in the CNS of treatment and control groups.

Finally, we evaluated whether MDP modulated microglial response by measuring Iba-1 protein levels. Iba1 protein levels in the CNS showed no significant difference between the treatment and the control groups confirming that MDP regulates specifically systemic myeloid cell infiltration in EAE (Fig. 4n). Together with the clinical scores, these results indicate that MDP significantly delayed EAE onset via the regulation of infiltrating monocytes and some other leukocytes with no evidence of altering microglia.

NOD2 Receptor Plays a Critical Role in MDP-Dependent Immune Modulation and EAE Resistance

Lessard and colleagues recently reported the critical role of NOD2 in mediating the conversion of Ly6C^{high} into LyC6^{low} monocytes [25]. To further address the role of the NOD2 receptor in MDP-mediated EAE resistance, EAE was induced in both WT and NOD2$^{-/-}$ mice, and they were then injected with either saline or MDP every 2 days (Fig. 5a). In contrast to WT mice treated with MDP, MDP treatment in NOD2$^{-/-}$ mice did not significantly delay EAE onset compared to WT–vehicle and NOD2$^{-/-}$–vehicle mice (Fig. 5b). NOD2$^{-/-}$ mice treated with MDP showed no significant weight changes and disease incidence than those of the control groups (Fig. 5c and d). Additionally, we only found significant differences in means of onset day and maximum score in WT mice but not NOD2$^{-/-}$ mice treated with MDP (Table 3). Altogether, the statistical analysis of clinical scores, weight changes, and disease incidences as well as means of onset day and maximum score, demonstrated a key role of NOD2 receptors in MDP-mediated EAE resistance. More importantly, these observations were further supported by the FACS results at 21 days after immunization. Indeed, MDP treatment in NOD2$^{-/-}$ mice did not show the same immune modulations as we observed in WT mice treated with MDP. As expected, MDP administrations modulated the number of Ly6C^{high} and LyC6^{low} monocytes in WT mice at this time point. In contrast, NOD2$^{-/-}$ mice treated with MDP did not show a significant difference in the number of monocyte subsets (Fig. 5e and f). We also did not find a significant effect of MDP-mediated immune modulation on T-cell subsets in NOD2$^{-/-}$ mice (Fig. S4).

To confirm the role of NOD2 triggering in immune modulation and resistance in EAE, we triggered the NOD2 receptor in WT mice with another agonist very similar to MDP called N-glycolyl MDP (NG-MDP). NG-MDP shares a similar formula with MDP, with one difference that is having N-glycolylated in the formula in contrast to MDP that has N-

Table 2 EAE development before and after EAE onset in the treatment and control groups, respectively

Groups	Mean onset day	Mean score of maximal symptoms	Total days
EAE–vehicle	10.20 ± 0.37	1.3 ± 0.66	12
EAE–MDP	0****	0*	12

Representative of mean onset day and mean score of maximal symptoms, and total days in WT mice, at the timepoint that all mice in the control group are sick, and no mouse in the treatment group show any disease symptom. The treatment in the groups started before EAE onset. Data are presented as mean ± S.E.M. $****P < 0.0001$, $*P = 0.04$, Student's t test

acetylated. WT mice were induced EAE with the same protocol, and mice were treated with NG-MDP with a similar treatment regimen (Fig. 5a). NG-MDP administration exerted immune modulation on monocyte subsets similar to MDP. However, to reach the statistically significant difference between the treatment and control groups, we had to double the

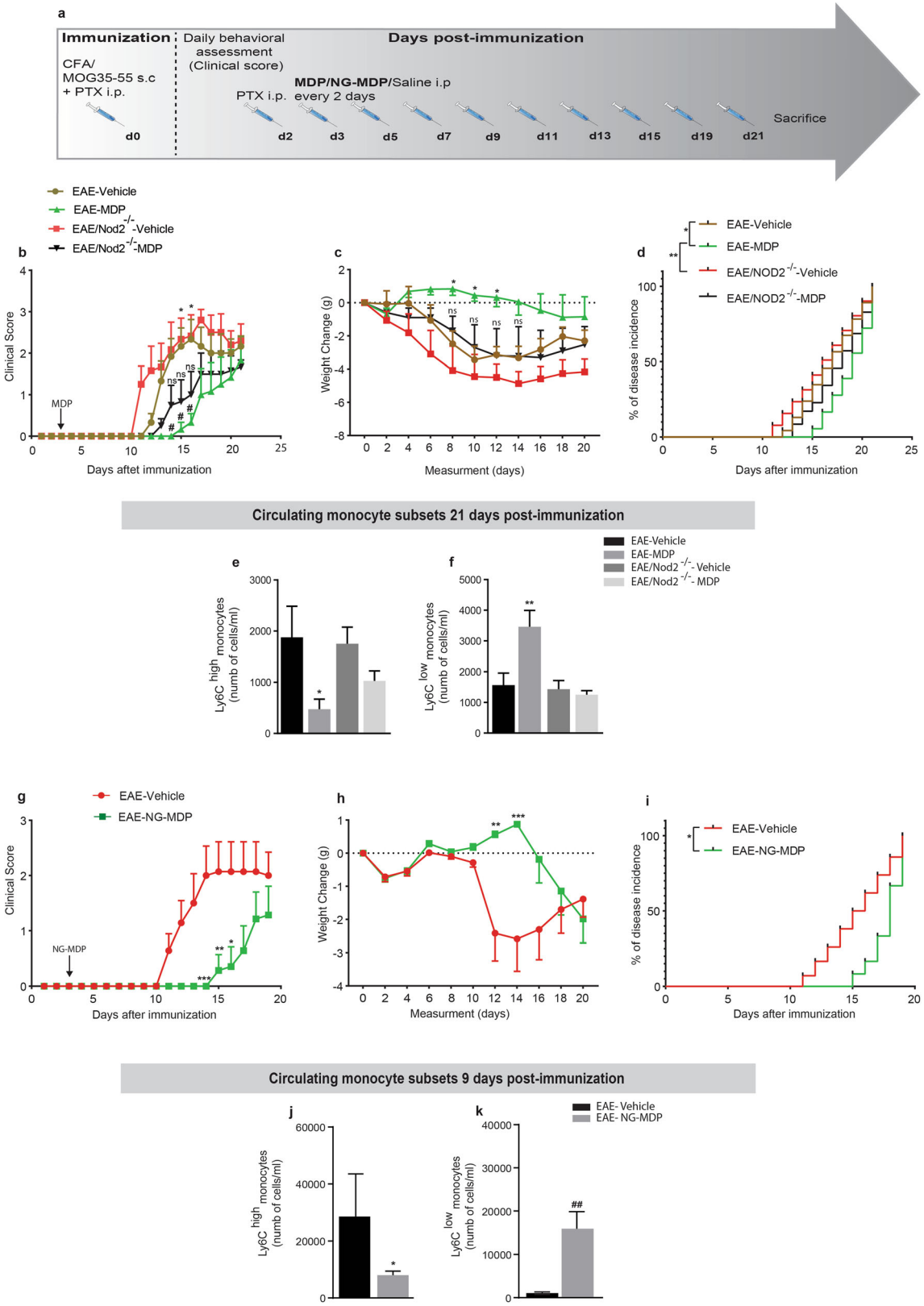

◀ **Fig. 5** The critical role of NOD2 receptor in MDP-dependent immune modulation and EAE resistance in mice. (a) Representative timeline of the entire protocol, including inducing EAE, MDP administrations in mice, $n = 6$ mice/group. (b) Clinical scores were determined daily after immunization. Data are expressed as the means ± SEM; days 14 to 16, $^{\#}P < \text{or} = 0.02$ *versus* EAE–vehicle, for days 15 and 16, $^{*}P = 0.02$ *versus* EAE–MDP, two-way ANOVA followed by Tukey's multiple comparisons test. (c) The variation of body weight has been expressed compared to the day of EAE induction (day 0) as mean ± SEM; $^{*}P < \text{or} = 0.03$ *versus* EAE–NOD2$^{-/-}$–vehicle, two-way ANOVA followed by Tukey's multiple comparisons test. (d) Percentage of disease incidence in mice treated with vehicle or MDP in all experimental groups. Data are expressed as the means ± SEM; $^{*}P = 0.002$ *versus* EAE–vehicle, $^{**}P = 0.004$ *versus* EAE–NOD2$^{-/-}$–vehicle, log–rank (Mantel–Cox) test. (e) Absolute count of blood Ly6C^{hi} monocytes by FACS following treatment with vehicle or MDP in all groups. Data are expressed as the means ± SEM; $^{*}P < \text{or} = 0.038$ *versus* EAE–WT–vehicle, one-way ANOVA with Tukey's multiple comparisons test. (f) Absolute count of blood Ly6C^{low} monocytes by FACS following treatment with vehicle or MDP in groups. Data are expressed as the means ± SEM; $^{**}P < \text{or} = 0.008$ *versus* EAE–WT–vehicle, one-way ANOVA with Tukey's multiple comparisons test. (G) Clinical scores of WT mice treated with vehicle ($n = 7$) or treated with NG-MDP ($n = 7$) were determined daily after immunization. Data are expressed as the means ± SEM; $^{***}P = 0.0008$, $^{**}P = 0.007$, $^{*}P = 0.01$, two-way ANOVA followed by Tukey's multiple comparisons test. (H) Body weight changes measured after immunization in the treatment and control groups. Data are expressed as the means ± SEM; $^{**}P = 0.003$, $^{***}P = 0.002$, two-way ANOVA followed by Tukey's multiple comparisons test. (I) Percentage of disease incidence in mice treated with vehicle or NG-MDP in all experimental groups. Data are expressed as the means ± SEM; $^{*}P = 0.01$, log–rank (Mantel–Cox) test. (j) and (k) Absolute count of blood Ly6C^{hi} and Ly6C^{low} monocytes respectively following treatment with vehicle or NG-MDP in EAE mice as measured by FACS 1 week after MDP injections (9 days after immunization). Data are expressed as the means ± SEM; $^{*}P < 0.04$ *versus* EAE–vehicle, $^{\#\#}P < 0.005$ *versus* EAE–vehicle, Student's *t* test

dosage. In this protocol, we also observed that triggering the NOD2 receptor, and consequently, the immune modulation significantly delayed the onset of the EAE (Fig. 5g–i and Table 4). Similar to previous results, the delay on the onset of EAE was correlated with a significant decrease and increase in inflammatory and anti-inflammatory monocytes, respectively (Fig. 5j and k). Interestingly, NG-MDP administration did not show any partial (or tendency) modulation of T cells (Fig. S5), as we observed with the MDP treatment. Altogether, these results suggest a critical role of NOD2 receptors in MDP-mediated immune resistance and innate immune modulation in the EAE model.

Peripheral MDP Administration After the Onset of the Disease Exerts Strong Therapeutic Effects on EAE Mice

Next, the most critical question we asked was whether MDP administration after the onset of disease could exert therapeutic effects in EAE mice. To answer this question, mice with score 2 have been assigned to both treatment and control groups. Then, we administrated MDP for four consecutive days in the treatment group and then the injections were followed every 2 days (Fig. 6a). Clinical scores and weight changes showed that MDP administration in the progressive phase ameliorated the course of EAE and protected mice from disease progression (Fig. 6b and c). In addition, MDP treatment improved the mean maximum score (Table 5). Following four consecutive days of MDP administrations, we performed a FACS study on blood and found a significant reduction and increase in inflammatory and patrolling monocytes, respectively (Fig. 6d and e). Altogether, these results indicate MDP treatment after EAE onset exerts strong therapeutic effects that are associated with immune modulation on monocyte subsets.

Discussion

Critical roles of monocytes in MS pathologies make them important therapeutic targets. Here we performed *in vivo* studies of MDP immunomodulatory effects in cuprizone and EAE mouse models of MS. Here we showed that peripheral MDP administration converts Ly6C^{high} towards Ly6C^{low} monocytes in both cuprizone and EAE models. Although demyelination levels did not change in the cuprizone model, the results obtained from the EAE model are greatly promising. It is important to mention that although MDP may modulate

Table 3 EAE progression in WT and NOD2$^{-/-}$ mice treated with vehicle or MDP

Groups	Mean onset day	Mean score of maximal symptoms	Total days
EAE–vehicle	12.80 ± 0.37	2.333 ± 0.47	21
EAE–MDP	18.40 ± 1.24**	1.750 ± 0.21$^{\#\#}$	21
EAE/NOD2$^{-/-}$–vehicle	11.80 ± 0.80	2.900 ± 0.18	21
EAE/NOD2$^{-/-}$–MDP	15.80 ± 1.31	1.833 ± 0.55	21

Representative of mean onset day and mean score of maximal symptoms, and total days for protocol in EAE and EAE/NOD2$^{-/-}$ mice treated with saline or MDP. Data are presented as mean ± S.E.M. $^{**}P < \text{or} = 0.006$ *versus* EAE–vehicle and EAE/NOD2$^{-/-}$–vehicle, one-way ANOVA followed by Tukey's multiple comparisons test. $^{\#\#}P = 0.008$ *versus* EAE/NOD2$^{-/-}$–vehicle, one-way ANOVA (Brown-Forsythe and Welch's ANOVA tests) comparing results from each group to the control groups followed by a post hoc comparison using Dunnett's T3 multiple comparisons test

Table 4 EAE progression in WT mice treated with vehicle or NG-MDP before the onset of EAE

Groups	Mean onset day	Mean score of maximal symptoms	Total days
EAE–vehicle	11.60 ± 0.40	2.90 ± 0.10	20
EAE–NG–MDP	15.0 ± 0.70**	2.25 ± 0.47$^{P=0.08}$	20

Representative of mean onset day and mean score of maximal symptoms, and total days for protocol in EAE mice treated with saline or NG-MDP started before the onset of EAE. Data are presented as mean ± S.E.M. $^{**}P = 0.001$, Student's *t* test

monocyte subsets via indirect mechanisms, Lessard and colleagues have previously demonstrated that MDP acts directly on these cells, mainly converting inflammatory monocytes into anti-inflammatory monocytes [25].

We have shown that MDP-treated mice were highly resistant to EAE, which seemed mediated by monocyte subsets regulation. Indeed, clinical scores confirmed that MDP treatment significantly delayed disease onset and decreased disease incidence. These observations were correlated with significant reduction and increase in Ly6C^{high} and Ly6C^{low} monocytes, respectively, both in the circulation and the CNS (Fig. 7). Several previous studies have unraveled the crucial roles of monocyte subsets and monocyte-derived macrophages in EAE and MS. In particular, the rapid influx of Ly6C^{high} monocytes from the circulation or peripheral reservoirs resulting in the onset of EAE, as CCR2-deficient mice are resistant to EAE [33, 34]. Furthermore, numbers of Ly6C^{high} monocytes increase in the blood within 1 day after immunization in EAE

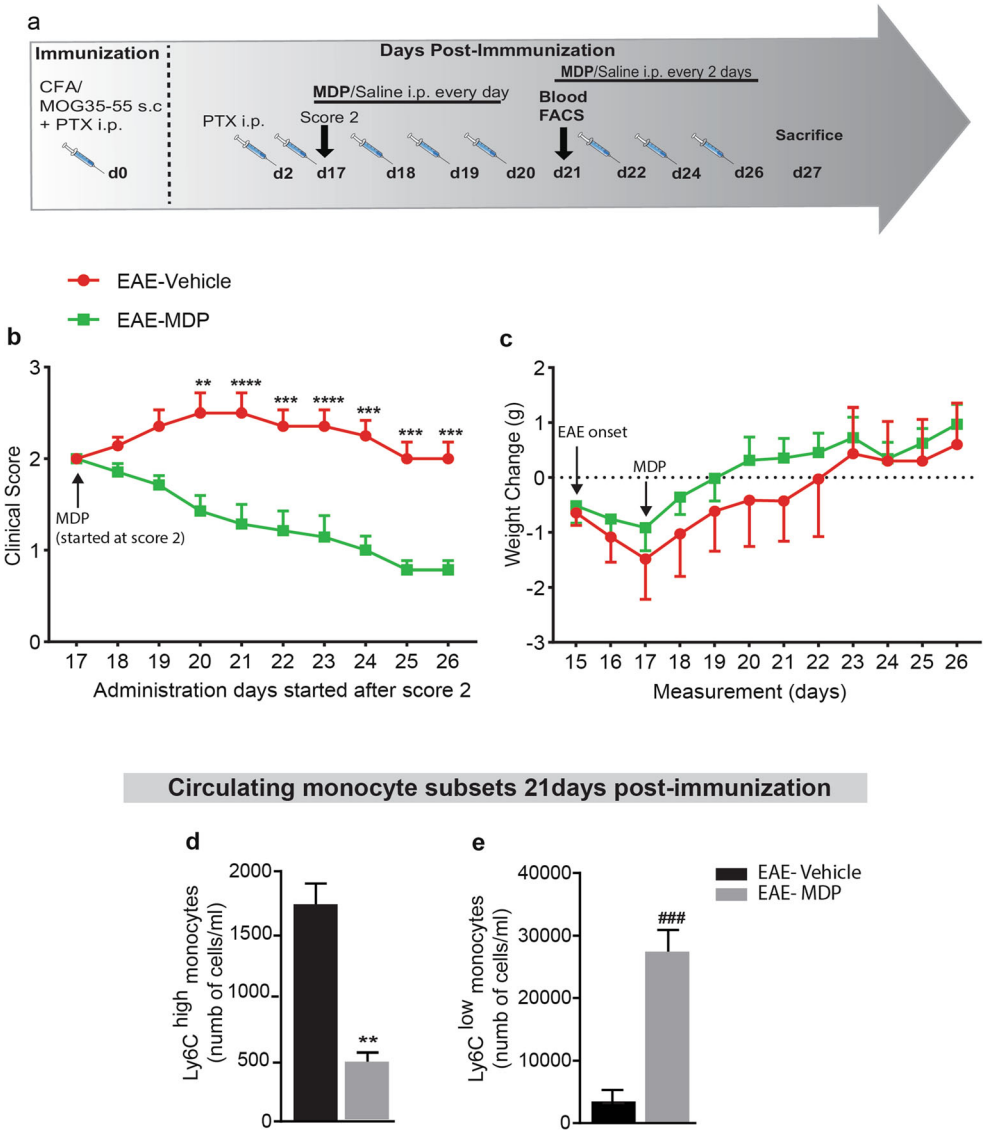

Fig. 6 MDP administration after the onset of the disease prevented EAE progression in mice. (a) Representative timeline of the entire protocol, including inducing EAE, MDP administrations, and FACS analysis in mice treated with vehicle ($n = 7$) or treated with MDP ($n = 7$). (b) Clinical scores of mice were determined daily after all mice selected with score 2. Data are expressed as the means ± SEM; $^{**}P = 0.01$, $^{***}P <$ or $= 0.0003$, $^{****}P < 0.0001$, two-way ANOVA followed by Tukey's multiple comparisons test. (c) Body weight changes measured after score 2 treatment in the treatment and control groups. Data are expressed as the means ± SEM. (d) and (e) Absolute count of blood Ly6C^{hi} and Ly6C^{low} monocytes respectively following treatment with vehicle or MDP in EAE mice as measured by FACS 1-week after MDP injections (21 days after immunization). Data are expressed as the means ± SEM; $^{**}P < 0.002$ *versus* EAE–vehicle, $^{###}P < 0.0002$ *versus* EAE–vehicle, Student's *t* test

Table 5 EAE progression in WT mice treated with vehicle or MDP started after EAE onset

Groups	Mean onset day	Mean score of maximal symptoms	Total days (after score 2)
EAE–vehicle	15.57 ± 0.20	2.0 ± 0.18	10
EAE–MDP	15.43 ± 0.20	0.7 ± 0.10****	10

Representative of mean onset day and mean score of maximal symptoms, and total days after all mice selected with the same score, in this protocol treatment with saline or MDP started after EAE onset. Data are presented as mean ± S.E.M. ****$P < 0.0001$, Student's t test

mice [35]. Administration of silica dust or clodronate liposomes that drastically reduce circulating Ly6C^{high} monocytes [36] also reduces or prevents EAE progression [37, 38]. Additionally, dipyridamole administration, a medication used clinically for secondary prevention in stroke, showed inhibitory effects on the activation of proinflammatory myeloid cells [39]. The significance of MDP-mediated reduction in Ly6C^{high} monocytes is not limited to the production of proinflammatory cytokines and chemokines [16]. It is also related to their effects on antigen presentation that activates T cells [40] and generation of oxidative stress and other mediators of injury [41–44].

In parallel, our results indicated a significant increase in Ly6C^{low} monocyte population in peripheral circulation as well as the CNS. The role of Ly6C^{low} monocytes in EAE amelioration has been well documented in previous studies. Indeed, *ex vivo* activated anti-inflammatory monocytes suppressed ongoing severe relapsing in an experimental rat model of MS [45]. Additionally, therapeutic effects of glatiramer acetate (GA, copolymer-1, Copaxone), a drug approved for MS that increased anti-inflammatory monocytes, is also beneficial in the EAE model [46]. Our results are quite in line with these data that promoting anti-inflammatory monocytes suppresses EAE.

Modulation of monocyte subsets can modify the population of monocyte-derived macrophages in systemic organs as well as in the CNS. For example, Ly6C^{low} monocytes can include perivascular macrophages [47, 48]. Some studies reported that depletion of both perivascular and meningeal macrophages

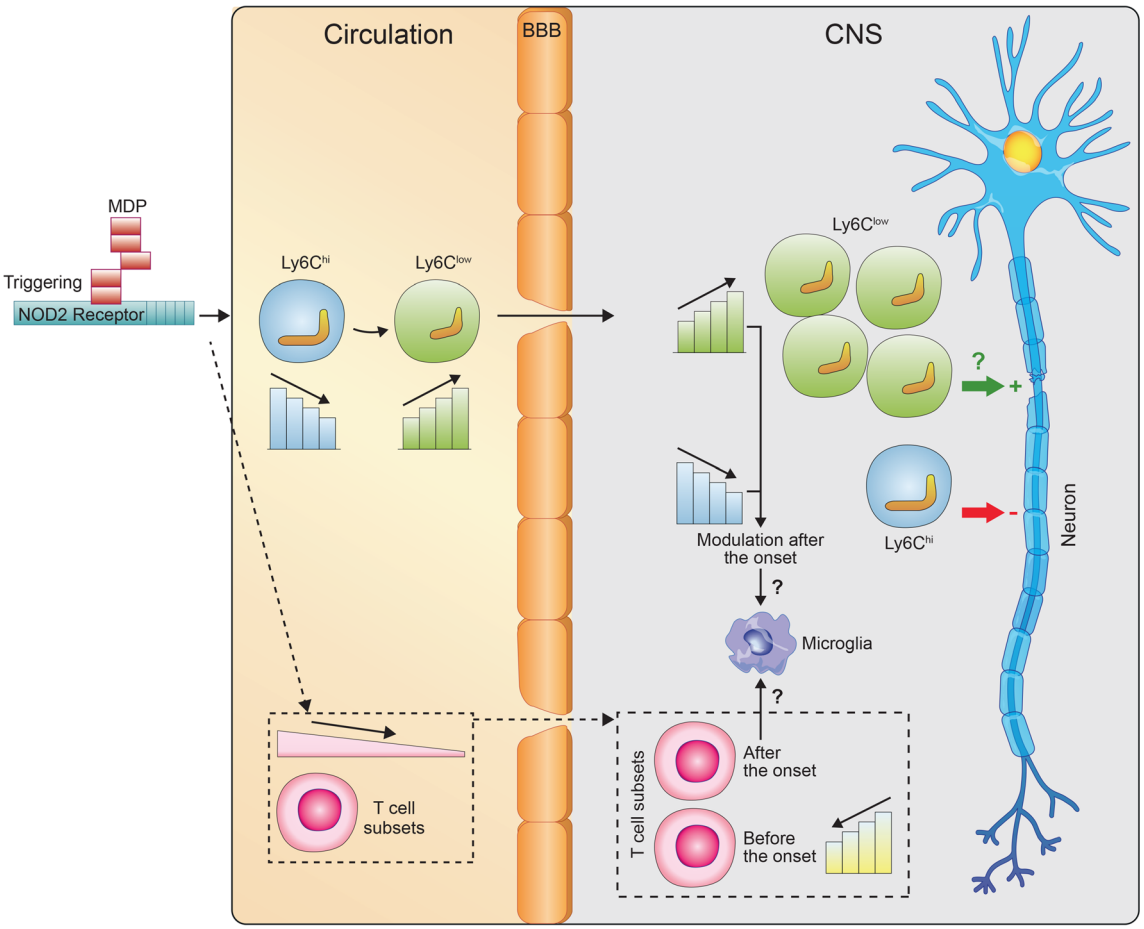

Fig. 7 Representative schematic illustration of monocyte modulation in the blood and the CNS in response to MDP administration in EAE mice

curtails EAE severity [49]. In parallel, immune cell activation and infiltration have been shown in the choroid plexus of MS patients [50, 51] and EAE animals [52]. In addition, choroid plexus macrophage–mediated inflammation in cerebrospinal fluid may directly impact meningeal and perivascular inflammation [53–55]. In this study, we did not directly assess monocyte-derived macrophages. Nevertheless, since MDP regulates both Ly6C^{high} and Ly6C^{low} monocytes as precursors of monocyte-derived macrophages, it is tempting to speculate that therapeutic effects of MDP might also regulate monocyte-derived macrophages indirectly. In this study, we also did not address the critical role of dendritic cells in the EAE onset. Although Lessard and colleagues showed that MDP treatment did not change the number of plasmacytoid and conventional splenic dendritic cells [25], future studies regarding possible effects of MDP on activation and production of cytokines from these cells are needed.

We have also demonstrated the critical role of NOD2 in MDP-mediated immunomodulatory and EAE resistance. In contrast to EAE mice treated with MDP, EAE–NOD2$^{-/-}$ mice treated with MDP did not show any significant difference in clinical scores, weight changes, disease incidence, mean onset day, and mean maximum score of maximal symptoms. More importantly, MDP treatment did not regulate monocyte subsets in EAE–NOD2$^{-/-}$ mice compared to EAE–WT mice. We further confirmed the role of NOD2 receptors by administrating another NOD2 agonist that is very similar to MDP. NG-MDP was also able to delay disease onset that was correlated with the modulation of monocyte subsets. Overall, these findings indicate that MDP does not mediate immune modulation on monocyte subsets and disease progression in the absence of NOD2 receptors.

Despite these exiting data, NOD2 agonists do not seem to have the same immunomodulatory potential since we had to double the dose of NG-MDP to reproduce the effects of MDP. Moreover, we did not find any modulation of T-cell subsets following the NG-MDP treatment, whereas MDP caused significant changes in T-cell subsets in EAE mice. These observations are quite interesting and may help us developing new drugs with great potential based on NOD2 agonist formulations.

The most striking results were obtained from the MDP administration after the EAE onset that prevented disease progression, and all mice were protected from the development of complete hind limb paralysis in the treatment group. The clinical scores were in line with the expected modulation of inflammatory and anti-inflammatory monocytes. The results we obtained from this protocol are critical. Nevertheless, future studies need to study MDP-mediated immune modulation in the progressive phase in other EAE models such as 2D2 mice that show a more severe EAE than nontransgenic littermates with a high frequency to develop spontaneous EAE [56].

In this study, we focused on immune modulation on monocyte subsets that were significantly changed upon MDP treatment. Whether MDP or other new synthetized NOD2 agonists could exert significant modulation on T-cell subsets is an open and interesting question that needs further studies. We only observed that MDP treatments significantly attenuated the influx of T-cell subsets into the CNS. Since less infiltrated T cells were not correlated with less T cells in the periphery, regulatory effects of MDP on monocyte subsets seem likely to contribute to the regulation of T-cell infiltration. In this regard, previous reports showed that monocyte/macrophage regulation has the ability to change T-cell subset infiltration [57, 58]. Of note, we also did not observe MDP-mediated immune modulation on T cells in NOD2$^{-/-}$ mice. Nevertheless, considering the marginal effect (at least in our experimental setup) of MDP treatment on T cells, we are not able to draw any conclusion, in general, regarding the exact role of NOD2 receptor in modulation of T cells, and in particular, about the role of MDP treatment in such modulation.

This study also raises questions about the effect of MDP on microglial activation and function. We identified no difference between Iba1 protein levels, suggesting that MDP might regulate only systemic myeloid cells, mainly Ly6C^{high} and Ly6C^{low} monocytes. However, this does not rule out an indirect effect of MDP on diverse microglial functions. Future studies using different time points after MDP administrations in different disease stages are needed to determine possible indirect effects of MDP specifically on microglia.

In conclusion, we have discovered therapeutic effects of MDP administration in an EAE mouse model of MS. We have demonstrated that MDP treatments delayed disease onset in the EAE model, which was accompanied by a significant reduction in the number of Ly6C^{high} cells in the blood, and the infiltrating cells into the CNS. Mechanistically, we have shown that the NOD2 receptor plays a critical role in MDP-mediated EAE resistance. More importantly, we have shown that MDP treatment after the onset of the EAE prevented disease progression. Medications that solely target specific monocyte subsets with mild immunomodulatory effects in the MS without triggering microglial activation are rare. We propose that NOD2-agonist-based medication might be a viable therapeutic approach for both the early and progressive phases of MS.

Supplementary Information The online version contains supplementary material available at https://doi.org/10.1007/s13311-020-00998-0.

Acknowledgments We thank Asmita Pradeep Yeola for helping in the EAE clinical scores. This work was supported by the Canadian Institutes in Health Research (CIHR) via the foundation scheme program and les Fonds de recherche du Québec- Santé (FRQS) via the research center funding grant. SR is supported by a Canadian Research Chair in Neuroimmunology. MR is a Junior-2 scholar of the Fonds de recherche du Quebec - Sante (FRQS).

Required Author Forms Disclosure forms provided by the authors are available with the online version of this article.

Compliance with Ethical Standards

Conflict of Interest The authors declare that they have no conflict of interest.**Supplementary Information** The online version contains supplementary material available at https://doi.org/10.1007/s13311-020-00998-0.

References

1. Girardin SE, Boneca IG, Viala J, Chamaillard M, Labigne A, Thomas G, et al. Nod2 is a general sensor of peptidoglycan through muramyl dipeptide (MDP) detection. J Biol Chem 2003;278(11):8869-72.
2. Willems MM, Zom GG, Meeuwenoord N, Khan S, Ossendorp F, Overkleeft HS, et al. Lipophilic Muramyl Dipeptide–Antigen Conjugates as Immunostimulating Agents. ChemMedChem. 2016;11(2):190-8.
3. Grimes CL, Ariyananda LDZ, Melnyk JE, O'Shea EK. The innate immune protein Nod2 binds directly to MDP, a bacterial cell wall fragment. J Am Chem Soc 2012;134(33):13535-7.
4. Kim Y-G, Kamada N, Shaw MH, Warner N, Chen GY, Franchi L, et al. The Nod2 sensor promotes intestinal pathogen eradication via the chemokine CCL2-dependent recruitment of inflammatory monocytes. Immunity. 2011;34(5):769-80.
5. Philpott DJ, Sorbara MT, Robertson SJ, Croitoru K, Girardin SE. NOD proteins: regulators of inflammation in health and disease. Nat Rev Immunol 2014;14(1):9.
6. Rahman MK, Midtling EH, Svingen PA, Xiong Y, Bell MP, Tung J, et al. The pathogen recognition receptor NOD2 regulates human FOXP3+ T cell survival. J Immunol. 2010;184(12):7247-7256.
7. Ogura Y, Bonen DK, Inohara N, Nicolae DL, Chen FF, Ramos R, et al. A frameshift mutation in NOD2 associated with susceptibility to Crohn's disease. Nature. 2001;411(6837):603.
8. Auffray C, Sieweke MH, Geissmann F. Blood monocytes: development, heterogeneity, and relationship with dendritic cells. Annu Rev Immunol 2009;27.
9. Guilliams M, Mildner A, Yona S. Developmental and functional heterogeneity of monocytes. Immunity. 2018;49(4):595-613.
10. Jakubzick C, Gautier EL, Gibbings SL, Sojka DK, Schlitzer A, Johnson TE, et al. Minimal differentiation of classical monocytes as they survey steady-state tissues and transport antigen to lymph nodes. Immunity. 2013;39(3):599-610.
11. Naert G, Rivest S. A deficiency in CCR2+ monocytes: the hidden side of Alzheimer's disease. J Mol Cell Biol 2013;5(5):284-93.
12. Sospedra M, Martin R. Immunology of multiple sclerosis. Annu Rev Immunol 2005;23:683-747.
13. Howell OW, Rundle JL, Garg A, Komada M, Brophy PJ, Reynolds R. Activated microglia mediate axoglial disruption that contributes to axonal injury in multiple sclerosis. J Neuropathol Exp Neurol 2010;69(10):1017-33.
14. Trebst C, Sørensen TL, Kivisäkk P, Cathcart MK, Hesselgesser J, Horuk R, et al. CCR1+/CCR5+ mononuclear phagocytes accumulate in the central nervous system of patients with multiple sclerosis. Am J Pathol 2001;159(5):1701-10.
15. Trapp BD, Peterson J, Ransohoff RM, Rudick R, Mörk S, Bö L. Axonal transection in the lesions of multiple sclerosis. N Engl J Med 1998;338(5):278-85.
16. King IL, Dickendesher TL, Segal BM. Circulating Ly-6C+ myeloid precursors migrate to the CNS and play a pathogenic role during autoimmune demyelinating disease. Blood. 2009;113(14):3190-7.
17. Ashhurst TM, van Vreden C, Niewold P, King NJC. The plasticity of inflammatory monocyte responses to the inflamed central nervous system. Cell Immunol 2014;291(1-2):49-57.
18. Saederup N, Cardona AE, Croft K, Mizutani M, Cotleur AC, Tsou C-L, et al. Selective chemokine receptor usage by central nervous system myeloid cells in CCR2-red fluorescent protein knock-in mice. PLoS One 2010;5(10):e13693.
19. Waschbisch A, Schröder S, Schraudner D, Sammet L, Weksler B, Melms A, et al. Pivotal role for CD16+ monocytes in immune surveillance of the central nervous system. J Immunol 2016;196(4):1558-67.
20. Fabriek BO, Van Haastert ES, Galea I, Polfliet MM, Döpp ED, Van Den Heuvel MM, et al. CD163-positive perivascular macrophages in the human CNS express molecules for antigen recognition and presentation. Glia. 2005;51(4):297-305.
21. Fani Maleki A, Cisbani G, Plante M-M, Préfontaine P, Laflamme N, Gosselin J, et al. Muramyl dipeptide-mediated immunomodulation on monocyte subsets exerts therapeutic effects in a mouse model of Alzheimer's disease. J Neuroinflammation 2020;17(1):218.
22. Deacon RM. Assessing nest building in mice. Nat Protoc 2006;1(3):1117-9.
23. Hui CW, St-Pierre M-K, Detuncq J, Aumailley L, Dubois M-J, Couture V, et al. Nonfunctional mutant Wrn protein leads to neurological deficits, neuronal stress, microglial alteration, and immune imbalance in a mouse model of Werner syndrome. Brain Behav Immun 2018;73:450-69.
24. Lampron A, Larochelle A, Laflamme N, Préfontaine P, Plante M-M, Sánchez MG, et al. Inefficient clearance of myelin debris by microglia impairs remyelinating processes. J Exp Med 2015;212(4):481-95.
25. Lessard A-J, LeBel M, Egarnes B, Préfontaine P, Thériault P, Droit A, et al. Triggering of NOD2 Receptor Converts Inflammatory Ly6C high into Ly6C low Monocytes with Patrolling Properties. Cell Rep 2017;20(8):1830-43.
26. Brunet A, LeBel M, Egarnes B, Paquet-Bouchard C, Lessard AJ, Brown JP, et al. NR4A1-dependent Ly6Clow monocytes contribute to reducing joint inflammation in arthritic mice through Treg cells. Eur J Immunol 2016;46(12):2789-800.
27. Laflamme N, Rivest S. Toll-like receptor 4: the missing link of the cerebral innate immune response triggered by circulating gram-negative bacterial cell wall components. FASEB J 2001;15(1):155-63.
28. Laflamme N, Lacroix S, Rivest S. An essential role of interleukin-1β in mediating NF-κB activity and COX-2 transcription in cells of the blood–brain barrier in response to a systemic and localized inflammation but not during endotoxemia. J Neurosci 1999;19(24):10923-30.
29. Döring A, Sloka S, Lau L, Mishra M, van Minnen J, Zhang X, et al. Stimulation of monocytes, macrophages, and microglia by amphotericin B and macrophage colony-stimulating factor promotes remyelination. J Neurosci 2015;35(3):1136-48.
30. Michaud J-P, Bellavance M-A, Préfontaine P, Rivest S. Real-time in vivo imaging reveals the ability of monocytes to clear vascular amyloid beta. Cell Rep 2013;5(3):646-53.
31. Laflamme N, Cisbani G, Préfontaine P, Srour Y, Bernier J, St-Pierre M-K, et al. mCSF-induced microglial activation prevents myelin loss and promotes its repair in a mouse model of multiple sclerosis. Front Cell Neurosci 2018;12:178.
32. Berard JL, Wolak K, Fournier S, David S. Characterization of relapsing–remitting and chronic forms of experimental autoimmune encephalomyelitis in C57BL/6 mice. Glia. 2010;58(4):434-45.
33. Fife BT, Huffnagle GB, Kuziel WA, Karpus WJ. CC chemokine receptor 2 is critical for induction of experimental autoimmune encephalomyelitis. J Exp Med 2000;192(6):899-906.

34. Izikson L, Klein RS, Luster AD, Weiner HL. Targeting monocyte recruitment in CNS autoimmune disease. Clin Immunol 2002;103(2):125-31.
35. Mishra MK, Wang J, Silva C, Mack M, Yong VW. Kinetics of proinflammatory monocytes in a model of multiple sclerosis and its perturbation by laquinimod. Am J Pathol 2012;181(2):642-51.
36. Mildner A, Mack M, Schmidt H, Brück W, Djukic M, Zabel MD, et al. CCR2+ Ly-6Chi monocytes are crucial for the effector phase of autoimmunity in the central nervous system. Brain. 2009;132(9): 2487-500.
37. Brosnan C, Bornstein M, Bloom B. The effects of macrophage depletion on the clinical and pathologic expression of experimental allergic encephalomyelitis. J Immunol 1981;126(2):614-20.
38. Huitinga I, Van Rooijen N, De Groot C, Uitdehaag B, Dijkstra C. Suppression of experimental allergic encephalomyelitis in Lewis rats after elimination of macrophages. J Exp Med 1990;172(4): 1025-33.
39. Sloka S, Metz LM, Hader W, Starreveld Y, Yong VW. Reduction of microglial activity in a model of multiple sclerosis by dipyridamole. J Neuroinflammation 2013;10(1):855.
40. Benveniste EN. Role of macrophages/microglia in multiple sclerosis and experimental allergic encephalomyelitis. J Mol Med 1997;75(3):165-73.
41. Nikić I, Merkler D, Sorbara C, Brinkoetter M, Kreutzfeldt M, Bareyre FM, et al. A reversible form of axon damage in experimental autoimmune encephalomyelitis and multiple sclerosis. Nat Med 2011;17(4):495.
42. Mossakowski AA, Pohlan J, Bremer D, Lindquist R, Millward JM, Bock M, et al. Tracking CNS and systemic sources of oxidative stress during the course of chronic neuroinflammation. Acta Neuropathol 2015;130(6):799-814.
43. Van Horssen J, Witte ME, Schreibelt G, De Vries HE. Radical changes in multiple sclerosis pathogenesis. Biochim Biophys Acta (BBA) - Mol Basis Dis. 2011;1812(2):141-50.
44. Yamasaki R, Lu H, Butovsky O, Ohno N, Rietsch AM, Cialic R, et al. Differential roles of microglia and monocytes in the inflamed central nervous system. J Exp Med 2014;211(8):1533-49.
45. Mikita J, Dubourdieu-Cassagno N, Deloire MS, Vekris A, Biran M, Raffard G, et al. Altered M1/M2 activation patterns of monocytes in severe relapsing experimental rat model of multiple sclerosis. Amelioration of clinical status by M2 activated monocyte administration. Mult Scler J 2011;17(1):2-15.
46. Weber MS, Prod'homme T, Youssef S, Dunn SE, Rundle CD, Lee L, et al. Type II monocytes modulate T cell–mediated central nervous system autoimmune disease. Nat Med 2007;13(8):935.
47. Sorokin L. The impact of the extracellular matrix on inflammation. Nat Rev Immunol 2010;10(10):712.
48. Agrawal SM, Williamson J, Sharma R, Kebir H, Patel K, Prat A, et al. Extracellular matrix metalloproteinase inducer shows active perivascular cuffs in multiple sclerosis. Brain. 2013;136(6):1760-77.
49. Greter M, Heppner FL, Lemos MP, Odermatt BM, Goebels N, Laufer T, et al. Dendritic cells permit immune invasion of the CNS in an animal model of multiple sclerosis. Nat Med 2005;11(3):328.
50. Vercellino M, Votta B, Condello C, Piacentino C, Romagnolo A, Merola A, et al. Involvement of the choroid plexus in multiple sclerosis autoimmune inflammation: a neuropathological study. J Neuroimmunol 2008;199(1-2):133-41.
51. Engelhardt B, Wolburg-Buchholz K, Wolburg H. Involvement of the choroid plexus in central nervous system inflammation. Microsc Res Tech 2001;52(1):112-29.
52. Brown DA, Sawchenko PE. Time course and distribution of inflammatory and neurodegenerative events suggest structural bases for the pathogenesis of experimental autoimmune encephalomyelitis. J Comp Neurol 2007;502(2):236-60.
53. Bragg D, Boles J, Meeker R. Destabilization of neuronal calcium homeostasis by factors secreted from choroid plexus macrophage cultures in response to feline immunodeficiency virus. Neurobiol Dis 2002;9(2):173-86.
54. Bragg D, Hudson L, Liang Y, Tompkins M, Fernandes A, Meeker R. Choroid plexus macrophages proliferate and release toxic factors in response to feline immunodeficiency virus. J Neurovirol 2002;8(3):225-39.
55. Vernet-der Garabedian B, Lemaigre-Dubreuil Y, Mariani J. Central origin of IL-1β produced during peripheral inflammation: role of meninges. Mol Brain Res 2000;75(2):259-63.
56. Procaccini C, De Rosa V, Pucino V, Formisano L, Matarese G. Animal models of multiple sclerosis. Eur J Pharmacol 2015;759: 182-91.
57. Tran EH, Hoekstra K, van Rooijen N, Dijkstra CD, Owens T. Immune invasion of the central nervous system parenchyma and experimental allergic encephalomyelitis, but not leukocyte extravasation from blood, are prevented in macrophage-depleted mice. J Immunol 1998;161(7):3767-75.
58. Bauer J, Huitinga I, Zhao W, Lassmann H, Hickey WF, Dijkstra CD. The role of macrophages, perivascular cells, and microglial cells in the pathogenesis of experimental autoimmune encephalomyelitis. Glia. 1995;15(4):437-46.